Check for updates

Original article

Institution of MECHANICAL ENGINEERS
Journal of PROCESS MECHANICAL ENGINEERING

Proc IMechE Part E:
J Process Mechanical Engineering
2020, Vol. 234(6) 673–683
© IMechE 2020
Article reuse guidelines:
sagepub.com/journals-permissions
DOI: 10.1177/0954408920938614
journals.sagepub.com/home/pie
SAGE

Variation and artificial neural network prediction of profile areas during slant type taper profiling of triangle at different machining parameters on Hastelloy X by wire electric discharge machining

IV Manoj and S Narendranath

Abstract

In the present research work, an in-house developed fixture is used to achieve taper profiles which avoids the disadvantages in convention tapering operation in wire electric discharge machining like wire bend, inaccuracies in taper, insufficient flushing, guide wear etc. A simple triangular profile was machined at 0°, 15° and 30° slant/taper angles. These taper profile areas are investigated for various machining parameters like wire guide distance, corner dwell time, wire offset and cutting speed override. It is observed that as the wire guide distance and cutting speed override increases, the profile area decreases. Whereas in case of wire offset, as offset increases the profile areas also increase. The corner dwell time parameter do not effect on the profile area. The taper profile areas measured highest at 30° followed by 15° and 0° slant angles. This is due to the workpiece placed at different angles during machining with the aid of fixture to obtain taper profile. The taper angle represents the angularity of slant triangular profiles. As the slant angle increases the variation in taper error also increases due to higher wire vibration. An artificial neural network model is developed for the prediction of these areas at a different slant angle. The model is validated experimentally where the errors in prediction ranged from 1% to 9%. In conclusion, it can be noticed that the machining parameters and slant angle influence on profiles irrespective of their dimensions.

Keywords

Slant type taper fixture, Hastelloy X, triangular slant profile, taper angle, profile area, artificial neural network

Date received: 28 February 2020; accepted: 6 June 2020

Introduction

Wire electric discharge machining (WEDM) is a precision machining technique that is used to generate complex shapes with varying hardness. Many materials like titanium alloys, nickel based alloys, metal matrix composites, ceramics can be machined using WEDM.[1–4] These components have application in the manufacture of precision parts like injection mould dies, blanking dies, injection nozzles etc.[5–7] The traditional guide adjustment mechanism for tapering causes the wire to bend which increases wire cut, causes guide wear, incomplete flushing, etc. As the wire is flexible, it is subjected to deformation and many other parameters also cause imprecisions during machining.[8–10] Many researchers like Yan et al.[11], Martowibowo et al.[12], Manoj et al.[13] and Sanchez et al.[14] have tried different innovative methods to avoid drawbacks of bending during the tapering process in WEDM by introducing new mechanisms and materials in the guide system, fixtures for taper machining. Plaza et al.[15] proposed DOE based and numerical models to predict angular error in tapering by WEDM. These models not only reduced trial and error experiments but the angular error was reduced to below 3'45" in 75% cases. Nayak et al.[16] have optimized tapering for a geometrical test part profile machined by WEDM using bat algorithm. The artificial neural network (ANN) used

Department of Mechanical Engineering, National Institute of Technology Karnataka, Surathkal, India

Corresponding author:
IV Manoj, Department of Mechanical Engineering, National Institute of Technology Karnataka, NH 66, Srinivasnagar, Surathkal, Mangalore 575025, India.
Email: vishalmanojvs@gmail.com

for finding a relationship between input and output parameters so that accuracy and performance characteristics can be obtained.

Sarkar et al.[17] formulated a model to enhance profile accuracy by compensating for measuring gap force intensity and wire lag in a cylindrical profile. It was concluded that the level of inaccuracy was higher for radius jobs where higher accuracies are required. Werner[18] explored a method in machining curvilinear profiles on wire-electric discharge machines. The optimal machining parameters were found by modern CAD/CAM systems and tool travel study.

Mishra et al.[19] have explored through-hole operation in Inconel using hollow (tubular) copper tool electrode. It was observed that an increase in pulse-on time has resulted in an increase in the SR, SCD, circularity, and WLT. Sharma et al.[20] have machined turbine disk profile using WEDM where the effects of machining parameters were investigated on microstructure and surface topography. Selvakumar et al.[21] have used path modification strategy in order to improve the accuracy die corner considering controllable and uncontrollable machining parameters. They achieved an improvement by 35% of corner accuracy of the profile considering path modification.

Nain et al.[22] have investigated that backpropagation BP-ANN method was found accurate than fuzzy logic in the prediction of surface roughness and waviness in a WEDM machined profile. Singh and Mishra[23] have highlighted that the backpropagation neural network (BPNN) in ANN was an effective tool for the prediction of surface roughness compared to the RSM model. Ming et al.[24] have reported ANN modelling using BPNN with the mean squared error was suitable in the prediction of surface roughness and material removal rate.

From the literature, it can be illustrated that profile features like accuracy, profile dimension, angle are influenced by the manufacturing parameters. The increasing applications also demand dimensional accuracy in oblique/taper components and many materials can only be machined precisely by WEDM. There were many problems with conventional tapering in WEDM and many parameters still have to be explored. In this paper, the triangular profile areas of 1mm and 5mm, taper angle are considered. A unique fixture is used to machine taper profiles at 0°, 15°, and 30° slant angles on Hastelloy X. This slant type taper fixture eliminates disadvantages during tapering in WEDM giving taper surface. Effects of uncharted WEDM input parameters like wire guide distance (α), corner dwell time (β), wire offset (γ) and cutting speed override (δ) on the profiles areas were studied. Different slant triangular profiles were machined on Hastelloy X using L_{16} Taguchi's orthogonal experiments for different input combinations. The effect of taper angle with different input parameters on slant profile area was studied after machining. The ANN is adopted to predict the areas of all the 1mm and 5mm profiles at different slant angles for various input parameters.

Material and method

Material

Hastelloy X is a nickel superalloy which derived from the first letters of the words, Haynes Stellite Alloy. It is a nickel-chromium-iron-molybdenum alloy used in many applications such as turbine combustion cans and ducting, heat-treating equipment, spray bars, flame holders, furnace rolls, furnace baffles, etc. It has excellent weldability and formability which eases the fabrication process. The Hastelloy X plate of 260mm×22mm×10mm was used for triangular profiling. It was subjected to full annealing at 1175°C (2145F) and holding time of 1h per inch of the section before machining.[25] The material composition was confirmed by Energy Dispersive X-Ray Analysis (EDX). Figure 1 shows the elements and their percentage weight composition present in the material.

Experimental details

In the WEDM process, sparks are generated between the wire and workpiece due to voltage difference which cuts the material to the desired shape. The dielectric fluid cools the workpiece and flushes the debris outside the machining area. The triangular profile to be machined was programmed using ELPULS CNC software. The necessary NC codes were generated based on machining conditions. The generated codes were exported to Electronica 'ELPULS 15 CNC WEDM' which was used to perform machining. The Zinc coated copper wire electrode of 0.25mm and water as dielectric fluid was employed through the experimental. The machining was performed on the Hastelloy X workpiece at different slant angles as shown in the Figure 2(a). The slant machining was achieved by the unique fixture that is made of aluminium H9. The workpiece was fixed to the angle plate which would be rotated for the required slant angle. The whole fixture is fixed on the table of WEDM. As the angle increases the cutting thickness also increases. Figure 2(c) shows the experimental outline followed in the present investigation.

Characterization techniques

In the present study, the cutting speed was calculated as an average of instantaneous speeds recorded during the machining of the profile. The 'JEO JSM-6368OLA' scanning electron microscope (SEM) was employed to record images of 1mm triangle. The Image J software was used to measure the areas of 1mm triangle. The coordinate measuring machine

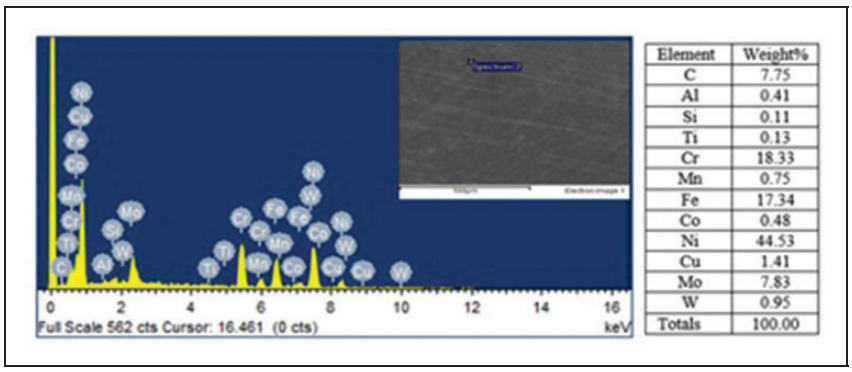

Figure 1. EDAX analysis of Hastelloy X.

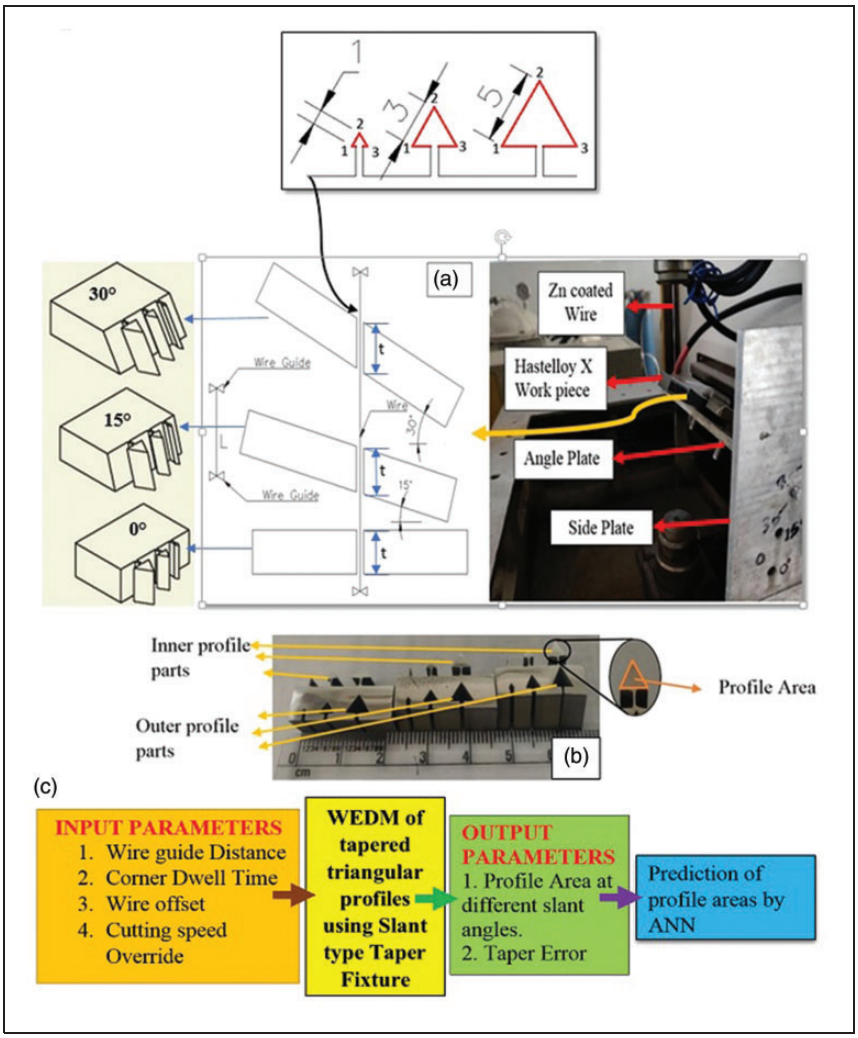

Figure 2. (a) Slant type taper machining and fixture. (b) Taper triangular profiles. (c) Experimental outline.

(CMM) 'TESA VISIO 200' was utilized to measure the edge distances and angle of machined components from which the area was calculated of 5mm triangle. The angle of slant machined component was also obtained using CMM from which the angular error was calculated. Artificial Neural Network with the aid of MATLAB was used in prediction of areas at different parameters for various angles.

Machining parameters

Table 1 shows the constant machining parameters used throughout the experimentation. These parameters were selected from the initial experiments carried out based on the workpiece and tool combinations. The effect of input parameters like wire guide distance, corner dwell time, wire offset and cutting

Table 1. Machining parameters.

Constant parameters				
EDM parameters	Settings			
Pulse off time (μs)	44			
Servo feed (mm/min)	20			
Wire feed (m/min)	6			
Pulse on time (μs)	115			
Servo voltage (V)	40			
Profiling parameters				
Wire guide distance (mm)(α)	40	50	60	70
	75	85	95	105
	100	110	120	130
Cutting speed override (%) (δ)	31	54	77	100
Wire offset (μm) (γ)	0	40	80	120
Corner dwell time (s) (β)	0	33	66	99

speed override was investigated. Taguchi's L_{16} orthogonal array was used in all the three slant angles and the triangular-shaped profiles were machined. The machining range (level) of each parameter for each slant angle was chosen based on the machining capabilities and initial experiments as shown in Table 1. The α parameter was kept minimal to minimize the vibration for different slant angles. At 0° to be 40mm-70mm, for 15° to be 75mm-105mm and for 30° to be 100mm-130mm as shown in Table 1. The triangular profiles of thickness 10mm that were machined for different slant angles are shown in Figure 2(b).

Results and discussion

Table 2 shows the 1 mm and 5 mm machined triangular areas at different slant angles. These areas were found to be smaller than the programmed dimensions because of the overcut and wire lag phenomenon.[17,26,27] The ANOVA and main effect plots were obtained from the measured profile areas. Table 3 shows the ANOVA for the areas recorded for different parameters at various slant angles. It can be concluded that the profile area was mostly influenced by the γ parameter. The γ parameter also contributed from 49% to 81% during slant profiling of both triangles. The next contributing parameter was α followed by δ parameter. It can be noticed that γ and α were the most significant factor in most of the cases. It can be observed from the ANOVA table and the main effects plots the β parameters contributes least on profile areas. The corner dwell time will make the wire dwell or stop in the corner for a fixed time at a co-ordinate during profiling. As the wire guide is stopped for a time at a specific point or coordinate the wire gets time to recover the lag. Hence, reducing the wire lag and eliminating the corner error.[28,29] The corner error always was formed in outer profile areas. The β parameter majorly influences mostly on corner outer profile areas.[30] This has a very low effect on the inner profiles during machining as found in ANOVA. From the main effects plot, we can observe that there are small variations of increase and decrease in β, these variations were due to the errors while machining. So β parameter can be neglected in further investigation.

Effect of γ on profile areas

From Figure 3(a), it can be concluded that as the γ parameter increases the profile areas also increases. This increases due to an increase in offset distance given to wire during profiling. The wire is moved to a fixed perpendicular distance from the programmed profile that leads to an increased profile area.[26,30] The amount and direction of shift of the wire can be controlled through part programming. Figure 3(a) shows a clear increase of profile areas as the γ parameter increases for 1mm triangle. It can be noticed that there was an increase in the case of 5mm triangle at 0μm to 40μm and 80μm to 100μm for 0°, 15° and 30° slant angles. This increase was observed due to the variation in wire vibration at higher values of offsets. As the wire offset values increase the wire have to cut the workpiece with a larger part of profile circumference. So wire vibration differs as compared to normal machining as stated by Habib and Okada.[31] The vibration also varies at different slant angle as explained in section 4 affecting the profile areas.

Effect of α on profile areas

The wire guide distance was the next contributing and significant parameter on profile areas. Figure 3(b) shows the main effects plot for 1mm and 5mm at different slant angles. As the α parameter increases the profile area decreases. This phenomenon of a decrease in the profile area was witnessed due to the increase in wire length (L). As the α increases the wire length (L) increases, the wire lag/wire deflection also escalates.[17] Hence, there would be an offset created that decreases the profile areas. This effect can be observed in 1mm triangle from 50mm to 70mm, 85mm to 105mm and 110mm to 130mm at 0°, 15° and 30° slant angles respectively. In the case of 5mm triangle, at 0° there is a clear decreasing trend as α increases. For 15°, it was viewed from 75mm to 85mm, 105mm to 95mm and for 30°, it can be noticed from 100mm to 120mm. There is a decrease at 40mm to 50mm at 0°, 75mm to 85mm at 15° and 100mm to 110mm at 30° for 1mm triangle. In 5mm triangle it was from 85mm to 95mm at 15° and 120mm to 130mm at 30° as in Figure 3(b). This variation was observed due to the stochastic vibrations of the wire during profiling.[32] These vibrations were caused because of the change in wire length. As the wire length increases the vibration also increases.[29,32]

Table 2. Slant areas at different parameters.

Sl. No.	α (mm)	β (s)	γ (μm)	δ (%)	Area of triangle in mm^2	
					1 mm	5 mm
0° slant angle						
1	40	0	0	31	0.27	9.101
2	40	33	40	54	0.293	9.412
3	40	66	80	77	0.37	9.81
4	40	99	120	100	0.434	10.007
5	50	0	40	77	0.25	8.904
6	50	33	0	100	0.153	8.557
7	50	66	120	31	0.422	10.02
8	50	99	80	54	0.316	9.597
9	60	0	80	100	0.231	9.359
10	60	33	120	77	0.362	9.492
11	60	66	0	54	0.205	8.338
12	60	99	40	31	0.236	9.019
13	70	0	120	54	0.354	9.518
14	70	33	80	31	0.305	9.361
15	70	66	40	100	0.169	8.209
16	70	99	0	77	0.111	8.106
15° slant angle						
1	75	0	0	31	0.28	10.75
2	75	33	40	54	0.339	11.004
3	75	66	80	77	0.393	12.087
4	75	99	120	100	0.466	12.189
5	85	0	40	77	0.291	10.819
6	85	33	0	100	0.19	10.371
7	85	66	120	31	0.473	12.709
8	85	99	80	54	0.336	11.802
9	95	0	80	100	0.309	11.484
10	95	33	120	77	0.395	11.328
11	95	66	0	54	0.243	10.328
12	95	99	40	31	0.248	10.48
13	105	0	120	54	0.389	11.805
14	105	33	80	31	0.366	11.59
15	105	66	40	100	0.203	9.71
16	105	99	0	77	0.145	9.782
30° slant angle						
1	100	0	0	31	0.37	11.686
2	100	33	40	54	0.383	11.99
3	100	66	80	77	0.481	12.09
4	100	99	120	100	0.521	12.416
5	110	0	40	77	0.33	11.66
6	110	33	0	100	0.237	10.781
7	110	66	120	31	0.519	12.801
8	110	99	80	54	0.403	12.124
9	120	0	80	100	0.379	11.755
10	120	33	120	77	0.454	11.72
12	120	99	40	31	0.252	11.383
13	130	0	120	54	0.341	11.161
14	130	33	80	31	0.495	11.491
15	130	66	40	100	0.412	12.001
16	130	99	0	77	0.284	10.997

Effect of δ on profile areas

From the main effects plot in Figure 3(c), it was noticed that as δ the increases the profile area decreases. As the δ parameter increases, the discharge energy also increases without changing the machining parameters. This mainly influences the cutting speed during machining. So as the δ increases the cutting speed also increases.[33] In 1mm triangle at 0°, 15° and from 54 to 100% at 30° slant angle, a clear decrease in the profile area were observed as the δ or cutting speed increases. Similarly, it was seen in the case of

Table 3. ANOVA for different slant angles.

			Area 1mm^2 triangle		Area 5 mm^2 triangle	
Sl. No.	Factor	DF	Sum of squares	% Contribution	Sum of squares	% Contribution
0° slant angle						
1	α	3	0.027	19.15	1.33	23.74
2	β	3	0.001	0.65	0.04	0.68
3	γ	**3**	**0.099**	**72.01**	**3.90**	**69.67**
4	δ	3	0.009	6.19	0.29	5.11
5	Error	3	0.003	2.01	0.05	0.80
15° slant angle						
1	α	3	0.019	13.98	1.79	15.47
2	β	3	0.002	1.40	0.08	0.71
3	γ	**3**	**0.107**	**77.71**	**8.85**	**76.64**
4	δ	3	0.006	4.22	0.51	4.39
5	Error	3	0.004	2.69	0.32	2.78
30° slant angle						
1	α	3	0.019	13.31	1.02	25.80
2	β	3	0.002	1.06	0.05	1.25
3	γ	**3**	**0.120**	**80.76**	**1.94**	**49.08**
4	δ	3	0.007	4.51	0.30	7.68
5	Error	3	0.001	0.35	0.64	0.16

The boldface values indicate that the 3rd parameter ie. (gamma parameter) was the major contributing factor in all the slant angles.

5mm triangle from 31%-77% at 0°, 31%-54% and 77%-100% at 15° and 31%-54% at 30° slant angle. This phenomenon was observed because at higher cutting speed the wire lag increases. This wire lag reduces the profile areas due to increases in the corner error in outer parts as observed by Selvakumar et al.[30] There are variations in decrease observed in 1mm triangle from 31%-54% at 30° and for 5mm triangle it was from 77% to 100% at 0°, 15°. As the variations were very feeble it may have been caused due to wire vibration resulting from sparking.[31,34]

Variation of profile areas at different slant angles

Figure 4 shows the variation of areas at different slant angles that were machined from various parameters. It can be observed that each parameter yields different areas although the cutting parameters such as pulse on, servo voltage etc. are kept constant. This phenomenon was because of change in input parameters, especially α, γ and δ. As the α increases the wire length also increases increasing the wire lag.[17] This wire lag influences the profile areas during machining. The γ parameter controls the amount and direction of shift of the wire this also leads to variation in areas of profile.[26] The effect of δ parameter was found to have an inverse relationship on the profile area compared with γ parameter as observed from the main effect plots. As each combination of these input parameters had wire lag, overcut and wire vibration.[31,34] The profiles areas for each parameter also defers irrespective of their dimensions. So the input parameters will contribute to the dimensional accuracy of the profile during machining. It can be noticed that profile areas cut at 30° have the highest areas followed by 15° and 0° slant angles. This increase was noticed throughout the experimental trials because as the slant angle increases the area for machining also increases.[13] This was due to availability of material as the workpiece tilted to increasing angle.

Variation of taper error of profile for different triangular dimensions

The dead errors which were errors present in the fixture before machining due to manufacturing approximations and errors. The actual error and the dead errors were also calculated by using equations (1) and (2).[13]

$$\text{Actual angle} = \text{CMM angle} - \text{Dead error} \quad (1)$$

$$\text{Taper Angular Error} = \text{Actual angle} - \text{Angle} \quad (2)$$

Figure 5 shows the variation of taper error with different experiments arranged in increasing order of their cutting speed. It can be seen that for 0° the least taper errors in degrees were -0.078° and -0.029°, at 15° errors were -0.028° and -0.036° and at 30° errors were 0.082° and 0.090° were calculated for 1mm and 5mm triangles respectively. Figure 5 shows the variation in taper error for 1mm triangle and 5mm triangle for different slant angles. It can be noticed that at 0° and 15° mostly intended to have negative errors, whereas 30° caused errors always towards the positive side. This variations in error were due to the manufacturing approximations during machining which was similar to results observed by Manoj et al.[13] As each parameter have

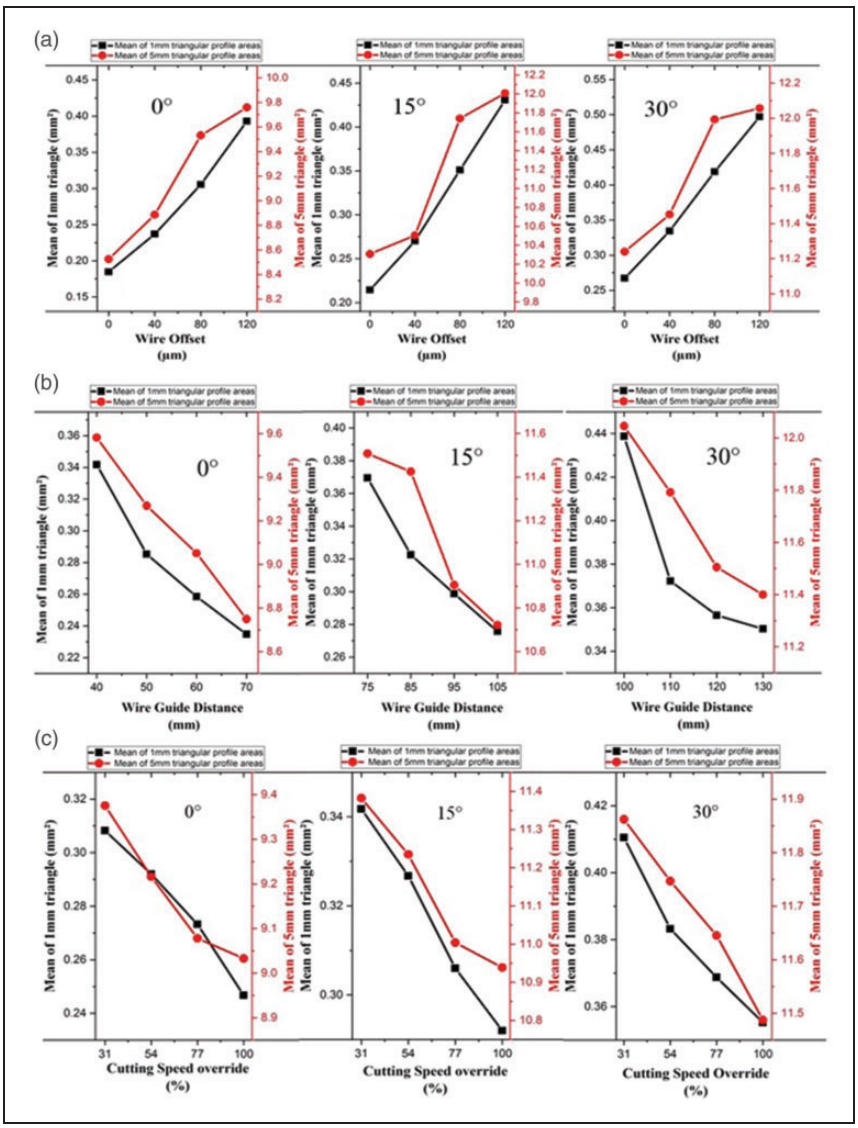

Figure 3. Main effect plots of (a) γ, (b) α, and (c) δ parameters.

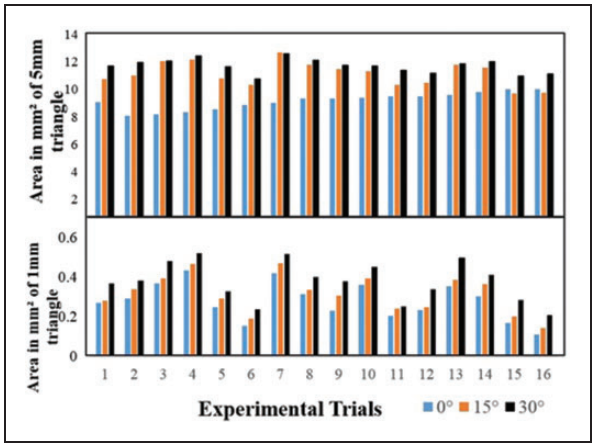

Figure 4. Variation in profile area at different slant angles.

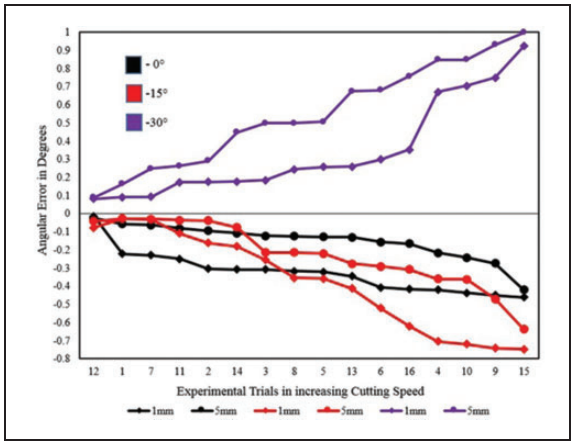

Figure 5. Variation of angular errors at different slant angles.

different cutting speeds due to varying machining parameters. This variation in errors mainly appears as the wire vibrations differs for each parametric combinations of α, γ and δ. The vibrations of wire were also caused due to sparking and discharging during profiling.[13,35] It was observed that as the discharge energy increases the cutting speed also increases.[33] We can observe that as the cutting speed increased

Table 4. Predicted and measured areas of triangles at different slant angles.

Slant angle (Degree)	Sl. no.	α (mm)	β (s)	δ (%)	Predicted area of triangle (mm^2)		Measured area of triangle in (mm^2)	
					1 mm	5 mm	1 mm	5 mm
0°	1	40	0	31	0.275	9.056	0.27	9.101
	2	40	40	54	0.288	9.279	0.293	9.412
	3	40	80	77	0.374	9.908	0.37	9.81
	4	40	120	100	0.436	9.994	0.434	10.007
	5	50	40	77	0.247	8.865	0.25	8.904
	6	50	0	100	0.160	8.567	0.153	8.557
	7	50	120	31	0.421	9.989	0.422	10.02
	8	50	80	54	0.319	9.651	0.316	9.597
	9	60	80	100	0.231	9.239	0.231	9.359
	10	60	120	77	0.362	9.504	0.362	9.492
	11	60	0	54	0.189	8.284	0.205	8.338
	12	60	40	31	0.231	9.051	0.236	9.019
	13	70	120	54	0.345	9.599	0.354	9.518
	14	70	80	31	0.311	9.379	0.305	9.361
	15	70	40	100	0.166	8.128	0.169	8.209
	16	70	0	77	0.108	8.168	0.111	8.106
15°	17	75	0	31	0.275	10.509	0.28	10.75
	18	75	40	54	0.337	11.103	0.339	11.004
	19	75	80	77	0.396	12.093	0.393	12.087
	20	75	120	100	0.464	12.211	0.466	12.189
	21	85	40	77	0.296	10.765	0.291	10.819
	22	85	0	100	0.184	10.248	0.19	10.371
	23	85	120	31	0.479	12.678	0.473	12.709
	24	85	80	54	0.340	11.692	0.336	11.802
	25	95	80	100	0.311	11.447	0.309	11.484
	26	95	120	77	0.391	11.309	0.395	11.328
	27	95	0	54	0.239	10.312	0.243	10.328
	28	95	40	31	0.253	10.573	0.248	10.48
	29	105	120	54	0.407	11.945	0.389	11.805
	30	105	80	31	0.367	11.518	0.366	11.59
	31	105	40	100	0.204	9.983	0.203	9.71
	32	105	0	77	0.149	9.747	0.145	9.782
30°	33	100	0	31	0.370	11.636	0.37	11.686
	34	100	40	54	0.379	12.069	0.383	11.99
	35	100	80	77	0.477	12.131	0.481	12.09
	36	100	120	100	0.520	12.411	0.521	12.416
	37	110	40	77	0.331	11.695	0.33	11.66
	38	110	0	100	0.241	10.753	0.237	10.781
	39	110	120	31	0.518	12.571	0.519	12.801
	40	110	80	54	0.407	12.150	0.403	12.124
	41	120	80	100	0.376	11.829	0.379	11.755
	42	120	120	77	0.458	11.590	0.454	11.72
	43	120	0	54	0.258	11.445	0.252	11.383
	44	120	40	31	0.329	11.204	0.341	11.161
	45	130	120	54	0.494	11.571	0.495	11.491
	46	130	80	31	0.411	11.949	0.412	12.001
	47	130	40	100	0.284	10.946	0.284	10.997
	48	130	0	77	0.205	11.103	0.21	11.111

errors also increased. This increase in taper error was due to the increase in wire vibration. The wire vibration increased as the discharge increased as observed by Puri and Bhattacharya[32,35] in there research. From the Figure 5, it can also be observed that the variation in error is maximum at 30° followed by 15° compared to 0° slant angles irrespective of profile dimensions. This trend was observed because as the angle of cut increases, the thickness of the workpiece also increases as shown in Figure 2(b). The vibration also increases as workpiece thickness increases at higher slant angles.[13,32,36] So 30° taper angles always were observed to have higher error variation than other taper angles. The phenomenon such as wire rupture, deflection, vibration, etc. also affects the geometrical accuracy.[27]

Table 5. Validation parameters for the optimum ANN model.

					1 mm triangle			5 mm triangle		
Sl. no.	α (mm)	β (s)	δ (%)	Slant angle (degree)	ANN predicted areas (mm^2)	Measured areas (mm^2)	Error (%)	ANN predicted areas (mm^2)	Measured areas (mm^2)	Error (%)
1	55	100	45	0°	0.374	0.410	8.77	9.776	9.570	2.15
2	80	180	80	0°	0.448	0.492	8.86	9.476	9.360	1.24
3	90	75	65	15°	0.274	0.268	2.39	7.569	8.010	5.51
4	120	150	50	15°	0.497	0.545	8.80	12.052	12.492	3.52
5	115	50	90	30°	0.346	0.334	3.47	11.690	12.712	8.04
6	145	130	70	30°	0.373	0.375	0.58	11.109	11.990	7.35

ANN prediction of profile areas at different slant angles

The 48 iterations were used from the design of experiments (DOE) for training, testing and validation of optimal ANN model. From the experiment, total sets were divided randomly into 70% for training, 15% for validation and 15% for testing the model by the software. Since BPNN integrated with Levenberg-Marquardt (LM) algorithm is most efficient as stated by Nain et al.,[22] similar network and algorithm combinations are used to train the neural network for prediction of areas. The profile areas recorded were normalized that ranged from -1 to 1 for training the network. The tansig function and the pureline functions were used for training the neural network. The mean square error (MSE) performance function was used for prediction of areas. Different hidden layer combinations were used to model to get the optimal architecture for prediction. The 4-9-1-1 ANN architecture was used in prediction of each case of 1mm and 5mm triangles. Table 4 shows the predicted and measured profile areas of triangles that were machined at various parameters for different slant angles.

Validation of the ANN model

The optimal model was obtained based on R-value in the regression plot. For validation, the input parameters are fed to the ANN model. The model was then made to simulate for prediction of output profile areas. The input parameters for validation were selected randomly from the experimental input parameters. Table 5 shows the validation input parameters, measured profile areas, predicted profile areas and error %. The highest error of 9% and the least was 1% calculated in predicted profile areas compared to experimental outputs.

Conclusion

Unlike convention taper machining the taper profiles were machined successfully without bending the wires with the aid of slant type taper fixture in WEDM. Effects of different input parameters and slant angle on profile features were explored. The following conclusions are drawn from the above research.

- Among the input parameters, α and γ were found to be the most significant factor affecting the profile area. As α increases the profile areas was found to decrease from 5% to 32% and for γ parameter, as it increases the profile areas also increased from 86% to 113%.
- In the cases of β and δ, the β parameters have no effect on profile areas. But as the δ parameter increases there was a decrement in the profile area from 20% to 13%.
- As the slant angle increases from 0° to 30°, the areas of the profile also increases. The increase in the profile area was found to be up to 20%-68%.
- In case of taper angle, as the slant angle increases from 0° to 30°, the variation in the error also escalates, due to the increase in wire vibration. The least and highest taper errors approximately -0.063° and 0.998° were recorded at 0° and 30° slant angle respectively.
- An optimal ANN model was modelled and validated through experiments. It was found that the errors were ranging from 1% to 9% in predicted profile areas.

Declaration of conflicting interests

The author(s) declared no potential conflicts of interest with respect to the research, authorship, and/or publication of this article.

Funding

The author(s) received no financial support for the research, authorship, and/or publication of this article.

ORCID iD

IV Manoj https://orcid.org/0000-0003-1556-3896

References

1. Okunkova A, Peretyagin P, Seleznyov A, et al. Characterization of material's defects after electrical discharge machining and research into their

technological parameters using vibroacoutstic diagnostics. *Adv Mater Lett* 2016; 7: 542–548.
2. Mouralova K, Prokes T and Benes L. Analysis of the oxide occurrence on WEDM surfaces in relation to subsequent surface treatments. *Proc IMechE, Part C: J Mechanical Engineering Science* 2019; 234: 721–733.
3. Kumar A, Kumar V and Kumar J. Investigation of machining characterization for wire wear ratio & MRR on pure titanium in WEDM process through response surface methodology. *Proc IMechE, Part E: J Process Mechanical Engineering* 2018; 232:108–126.
4. Abbas Al-Refaie. A proposed weighted additive model to optimize multiple quality responses in the Taguchi method with applications. *Proc IMechE, Part E: J Process Mechanical Engineering* 2013; 229: 168–178.
5. Uriarte L, Herrero A, Ivanov A, et al. Comparison between microfabrication technologies for metal tooling. *Proc IMechE, Part C: J Mechanical Engineering Science* 2006; 220: 1665–1676.
6. Pittman JFT. Computer-aided design and optimization of profile extrusion dies for thermoplastics and rubber: a review. *Proc IMechE, Part E: J Process Mechanical Engineering* 2016; 225: 280–321.
7. Mastud SA, Garg M, Singh R, et al. Recent developments in the reverse micro-electrical discharge machining in the fabrication of arrayed micro-features. *Proc IMechE, Part C: J Mechanical Engineering Science* 2011; 226: 367–384.
8. Kinoshita N, Fukui M and Fujii T. Study on wire-EDM: accuracy in taper-cut. *CIRP Ann* 1987; 36:119–122.
9. Chen Z, Zhang G and Yan HA. High-precision constant wire tension control system for improving workpiece surface quality and geometric accuracy in WEDM. *Precis Eng* 2018; 54: 51–59.
10. Tomura S and Kunieda M. Analysis of electromagnetic force in wire-EDM. *Precis Eng* 2009; 33: 255–262.
11. Yan H, Liu Z, Li L, et al. Large taper mechanism of HS-WEDM. *Int J Adv Manuf Technol* 2017; 90: 2969–2977.
12. Martowibowo SY and Wahyudi A. Taguchi method implementation in taper motion wire EDM process optimization. *J Inst Eng India Ser C* 2012; 93: 357–364.
13. Manoj IV, Joy R and Narendranath S. Investigation on the effect of variation in cutting speeds and angle of cut during slant type taper cutting in WEDM of Hastelloy X. *Arab J Sci Eng* 2020; 45: 641–651.
14. Sanchez JA, Plaza S, Ortega N, et al. Experimental and numerical study of angular error in wire-EDM taper-cutting. *Int J Adv Manuf Technol* 2008; 48: 1420–1428.
15. Plaza S, Ortega N, Sanchez JA, et al. Original models for the prediction of angular error in wire-EDM taper-cutting. *Int J Adv Manuf Technol* 2009; 44: 529–538.
16. Nayak BB and Mahapatra SS. Optimization of WEDM process parameters using deep cryo-treated Inconel 718 as work material. *Eng Sci Technol Int J* 2016; 19: 161–170.
17. Sarkar S, Sekh M, Mitra S, et al. A novel method of determination of wire lag for enhanced profile accuracy in WEDM. *Precis Eng* 2011; 35: 339–347.
18. Werner A. Method for enhanced accuracy in machining curvilinear profiles on wire-cut electrical discharge machines. *Precis Eng* 2016; 44: 75–80.
19. Mishra DK, Rahul, Datta S, et al. Through hole making by electro-discharge machining on Inconel 625 super alloy using hollow copper tool electrode. *Proc IMechE, Part E: J Process Mechanical Engineering* 2018; 233:348–370.
20. Sharma P, Chakradhar D and Narendranath S. Evaluation of WEDM performance characteristics of Inconel 706 for turbine disk application. *Mat Des* 2015; 88: 558–566.
21. Selvakumar G, Thiruppathi Kuttalingam K G, Selvaraj M, et al. Enhancing die corner accuracy using path modification strategy in wire electrical discharge machining of Monel 400. *Proc IMechE, Part C: J Mechanical Engineering Science* 2016; 232: 207–216.
22. Nain SS, Sihag P and Luthra S. Performance evaluation of fuzzy-logic and BP-ANN methods for WEDM of aeronautics superalloy. *Methods X* 2018; 5: 890–908.
23. Singh B and Misra JP. Surface finish analysis of wire electric discharge machined specimens by RSM and ANN modelling. *Measurement* 2019; 137: 225–237
24. Ming W, Hou J, Zhang Z, et al. Integrated ANN-LWPA for cutting parameter optimization in WEDM. *Int J Adv Manuf Technol* 2016; 84: 1277–1294.
25. Chandler H. *Heat treater's guide practices and procedures for nonferrous alloys* (Third printing). Cleveland: ASM International, 2006.
26. Kumar A, Kumar V and Kumar J. Semi-empirical model on MRR and overcut in WEDM process of pure titanium using multi-objective desirability approach. *J Braz Soc Mech Sci Eng* 2015; 37: 689–721.
27. Chen Z, Huang Y, Zhang Z, et al. An analysis and optimization of the geometrical inaccuracy in WEDM rough corner cutting. *Int J Adv Manuf Technol* 2014; 74: 917–929.
28. Yongqi F, Bryan NKA, Shing ON, et al. Influence analysis of dwell time on focused ion beam micromachining in silicon. *Sens Actuat* 2000; 79: 230–234.
29. Electronica India Ltd. Operating manual for ELPLUS 15 Ecocut (Retrieved by email from company) (2011, accessed 25 June 2011).
30. Selvakumar G, Kuttalingam KT and Prakash SR. Investigation on machining and surface characteristics of AA5083 for cryogenic applications by adopting trim cut in WEDM. *J Braz Soc Mech Sci Eng* 2018; 40: 1–8.
31. Habib S and Okada A. Experimental investigation on wire vibration during fine wire electrical discharge machining process. *Int J Adv Manuf Technol* 2016; 84: 2265–2276.
32. Puri AB and Bhattacharyya B. An analysis and optimisation of the geometrical inaccuracy due to wire lag phenomenon in WEDM. *Int J Mach Tool Manuf* 2003; 43: 151–159.

33. Manoj IV, Joy R, Narendranath S, et al. Investigation of machining parameters on corner accuracies for slant type taper triangle shaped profiles using WEDM on Hastelloy X. *IOP Conf Ser Mater Sci Eng* 2019; 591: 012022.
34. Habib S. Optimization of machining parameters and wire vibration in wire electrical discharge machining process. *Mech Adv Mater Mod Process* 2017; 3: 1–9.
35. Puri AB and Bhattacharyya B. Modelling and analysis of the wire tool vibration in wire cut EDM. *J Mater Process Tech* 2003; 141: 295–301.
36. Samanta A, Sekh M and Soumya S. Influence of different control strategies in wire electrical discharge machining of varying height job. *Int J Adv Manuf Technol* 2019; 100: 1299–1309.